Assessment of Reliability and Diagnostic Performance of Anterior Cruciate Ligament on Proton Density Weighted (PDW) Images using 2D TSE and 3D SPACE in MRI 3T.

[1,2]Almutiari Ali Dkheelallah A; [2]Nur Fahayu Omar; [3]Azlan Che Ahmad; [4*]Abubakar Danmaigoro; [5]Abdurahman Ibrahim Elmurr; [5]Haniyya Abdullah Alrehaily; [5]Turki Hamid Alrehaily; [2]Suraini Mohamad Saini

[1]Department of Radiology, Ministry of Health, Medina, Saudi Arabia

[2]Department of Radiology and Imaging, Faculty of Medicine and Health Sciences, Universiti Putra Malaysia, 43400, Serdang, Selangor, Darul Ehsan, Malaysia

[3]Department of Biomedical Imaging, Faculty of Medicine, Universiti Malaya, 59100, Kuala Lumpur

[4]Department of Veterinary Preclinical Sciences, Faculty of Veterinary Medicine, Universiti Malaysia Kelantan, Pengkalan Chepa,16100 Kota Bharu, Kelantan, Malaysia

[5]Medinah King Fahd Hospital, Medinah, Saudi Arabia

*Corresponding author: abubakar.dm@umk.edu.my

***Abstract*:** Knee derangements are becoming more common due to sudden biomechanical twisting of the limbs. MRI stands out as an effective non-invasive diagnostic tool compared to other methods offering high spatial resolution for visualizing complex knee anatomy. 3D SPACE offers advantages over the two-dimensional (2D) turbo spin-echo acquisition with multi-planar reformat using isotropic voxel acquisition, thus providing improved imaging quality for ACL injury detection. Limited studies have compared the diagnostic accuracy of 3D SPACE with the 2D turbo spin-echo sequence in detecting anterior cruciate ligament injuries. This study assesses the image quality and diagnostic performance of 3D SPACE and 2D TSE in ACL evaluation using a 3T MRI. A case-control study involved 60 individuals, divided into an injured-knee group and healthy patients between 2019 – and 2020 at King Fahad Hospital. All MRI acquisitions were performed on a 3T MRI scanner using a standard knee protocol. The study included 35 patients and 25 healthy participants. A significant difference ($p = 0.001$) in image sharpness between 2D PD and 3D PD in patients with knee injuries was observed with higher diagnostic accuracy of ACL among patients (AUC 0.973), which is statistically significant ($P < 0.001$) when compared between 3D PD SPACE to 2D PD sequence, with weighted kappa values of 0.740 and 0.784, respectively. Kappa agreement values indicated substantial agreement in 3D PD SPACE compared to 2D PD in cases of ACL knee injury. The results reveal that both sequences proved valuable diagnostic accuracy in detecting ACL injuries, with 3D SPACE offering enhanced isotropic resolution and multiplanar reformation capabilities, leading to improved visualization of the ACL, thus underscoring the importance of appropriate imaging technique selection for scan efficiency and clinical feasibility. This research contributes to the growing evidence that 3D PD SPACE sequences are beneficial, provide sufficient image quality in a short scan time, and are a reliable component of knee MRI.

***Keywords*:** 3D Space, Magnetic Resonance Imaging, Anterior Cruciate Ligament, Knee injury

Sustainable Development Goal: Good Health and Wellbeing

Background

Globally, the cases of knee injuries and tears are currently on the rise, which are mainly associated with a high incidence of cruciate ligament lesions [1]. Knee injury results from a direct blow with sudden twisting, causing the most common knee injuries. MRI has recently become essential for diagnosing subtle knee injuries, offering high spatial resolution to visualize the intricate anatomy of the knee [2]. The imaging tool delivers adequate accuracy for diagnosing cruciate ligament tears, as well as evaluating reconstructed ligaments, meniscal tears, and other knee conditions. Furthermore, MRI holds the potential to serve as an alternative to or replacement for diagnostic arthroscopy [3].

Over the years, Magnetic resonance imaging (MRI) technology has rapidly advanced development, ranging from the capacity and sectioning sequences deployed [4], [5]. Advances in system software and hardware have enabled fast imaging sequences, allowing for many techniques and applications not previously possible with conventional MRI [6]. Fast spin-echo sequences utilized in various MRI systems have a quicker acquisition time compared to conventional spin-echo methods [7]. MR knee protocols used in clinical practice typically involve a combination of 2D turbo spin-echo sequences acquired in multiple planes to assess the knee [8] with the assessment of ACL injuries usually employing two-dimensional (2D) MRI pulse sequences. This may explain the discrepancies as only one plane of a region of interest (ROI) is assessed compared to the three-dimensional (3D) images [9]. The 3D turbo spin-echo sequence can generate high-quality multi-planar images due to its isotropic voxel acquisition without slice gaps [10]. The 3D turbo spin-echo with sampling perfection with application-optimized contrast and various flip angle evolutions (SPACE) sequence is capable of producing T1-weighted (T1W), T2-weighted (T2W), or proton density-weighted (PDW) contrasts [4]. This technique captures 3D images with medium to high resolution in a reasonable acquisition time. The scan time of 3D SPACE can be reduced compared to the multi-planar 2D TSE since it can be reformatted into multi-plane reconstructions from a single acquisition. Most studies evaluating 3D spin-echo sequences on the knee have been conducted using 3T MRI [11], [12], [13]. Limited studies have assessed the diagnostic accuracy performance between 3D isotropic FSE and 2D TSE SPACE for detecting anterior cruciate ligament injuries [8]. The SPACE sequence offers a significant advantage by mimicking the contrast properties of conventional 2D TSE proton density-weighted acquisitions [11], [14], potentially replacing multiple conventional 2D acquisitions. This study aims to evaluate and compare the Proton Density Weighted image sharpness and diagnostic accuracy and performance of the anterior cruciate ligaments (ACL) among healthy subjects and patients with partial and complete tears of the ACL using 2D TSE and 3D TSE on 3T MRI at King Fahad Hospital. thus overcoming the long acquisition times by adopting the best sequence techniques, which are highly specific and sensitive in detecting Knee injury.

Materials and Methods

Study Design and Sampling

A case-control study design was used with the participants divided into two groups: the injured knee (patient) group and the non-injured knee group (healthy). All patients with an ACL injury only, experiencing dysfunction during daily activities or in sports, were screened by an orthopedic specialist for study eligibility between April 2019 and December 2021. Written informed consent was obtained, and images were acquired using the 3T MRI.

Study Population

The subjects were aged between 15 and 55 and scheduled to undergo a knee MRI examination at the Radiology Department of King Fahd Hospital in Madinah Munawara, Saudi Arabia. All anterior cruciate ligament rupture cases in the MRI unit were recorded and archived. Demographic data such as age, gender, suspected knee abnormalities, and clinical history were obtained from the patient records. The pregnant patients with previous knee surgery and those who underwent contrast-MRI were excluded. The healthy group consisted of patients from the Orthopaedic Clinic who were confirmed not to have a diagnosis of a current or previous ACL injury. The patient group consisted of patients with an ACL injury confirmed by MRI and clinical examination.

MRI protocol

The subjects were scanned using a 3T MRI machine (MAGNETOM Skyra, Siemens Healthineers, Erlangen, Germany) with a 15-element transmit/receive coil. The 2D PDW images of the knee were acquired in a sagittal view using a fat-suppressed (FS) sequence. These sequences were part of the knee MRI routine protocol at the hospital. Additionally, isotropic 3D PDW images were acquired using Sampling Perfection with Application-optimized Contrast using different flip angle Evolutions (SPACE) with the FS sequence. The MRI parameters and scanning times for both sequences are shown in Table 1.

Table 1 : Parameters for the knee MRI protocol

Sequence	2D TSE	3D SPACE
TR (ms)	3290	1470
TE (ms)	30	34
FOV (mm)	160 x 160	160 x 160
Slice thickness (mm)	3	0.45
Slice gap (%)	15	0
Matrix size	256 x 256	218 x 218
Signal averaging	2	1
Scan time (mins)	3:00	4:40

Baseline Clinical Assessment

All the patients with ACL injuries underwent the arthroscopic biopsy as a standard reference after an MRI examination. After taking a complete medical history and clinical assessment, including the Lachman test, Drawer test, and McMurray, the grinding tests evaluated the knee-associated structures. All arthroscopic protocols were done by a qualified and experienced orthopedic surgeon with expertise in knee surgery and more than half a decade of clinical practice. The ACL injury was grouped into two categories: partial and complete torn.

Data Analysis

Two fully trained radiologists with over ten years of experience in musculoskeletal imaging evaluated the ACL images' sharpness and diagnostic accuracy on 2D and 3D PDW images separately for both groups. The radiologists were unaware of the patient's diagnosis, age, and gender. They independently reviewed the images of both groups separately in two sessions, which were separated by two weeks to minimize recall bias. The 2D and 3D PDW image sets were offered randomly to the radiologists. This was to ensure that the 2D and 3D PDW image sets of the same patient were not reviewed in the same session. The image analysis was done by using the Siemens workstation with Syngo®

The sharpness in the margin of the ACL was graded with a 4-point scale; 0 = poor, 1= fair, 2 = good, and 3 = excellent for both sagittal 2D and 3D PDW images. Both radiologists graded the sharpness of the ACL fibers in both the healthy and patient groups (**Figure 1**). The ACL injuries were graded on a scale of 1–5; 1= normal, 2 = probably not a tear; 3 = indeterminate, 4 = partial tear and 5 = complete tear for both sagittal 2D and 3D PDW images. Both radiologists were unaware of the clinical data. First, both radiologists separately reviewed sagittal 2D and 3D PDW images. Then both radiologists graded the ACL injury-fibres in both the healthy and patient groups (**Figure 1**).

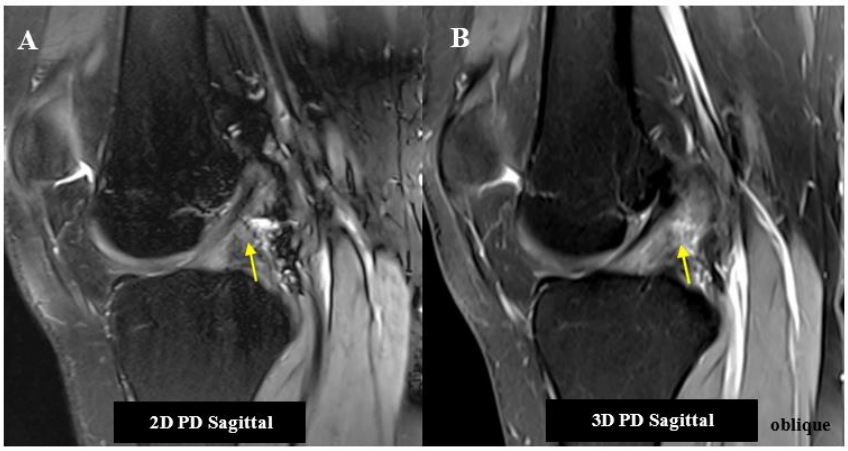

Figure 1: 2D (A) and 3D (B) PD sagittal images with fat suppression of the same patient. 2D PD image (A) revealed blurring of ACL fibres at its distal part, which can be seen intact at the 3D PD sagittal view (B) with adequate improvement in resolution along its entire course compared to the 2D PD image (A). The ACL fibres are sharper in the 3D PD image (score 3) than in the 2D PD image (score 1). The injury score was 5 for the 2D image and 4 for the

3D image

For the evaluation of the inter-observer agreement, the image sharpness and injury grading for each MRI sequence were calculated using kappa (κ) coefficients analysis. The image sharpness and ACL injury grading between 2D and 3D PDW images for each group also were compared using the one-way ANOVA test. The grading results between healthy and patient groups for each MRI sequence also were compared using the one-way ANOVA test. Paired t-test was used to assess the differences. Differences were significant if the p-value was less than 0.05.

The radiological diagnosis of ACL injury using both MRI sequences was correlated with arthroscopy. Receiver-operator characteristic (ROC) analysis was applied to assess the detection and diagnostic accuracy of ACL partial and complete tears on the 2D and 3D PDW images that were acquired using 2D TSE and 3D FS SPACE sequences (**Figure 2**).

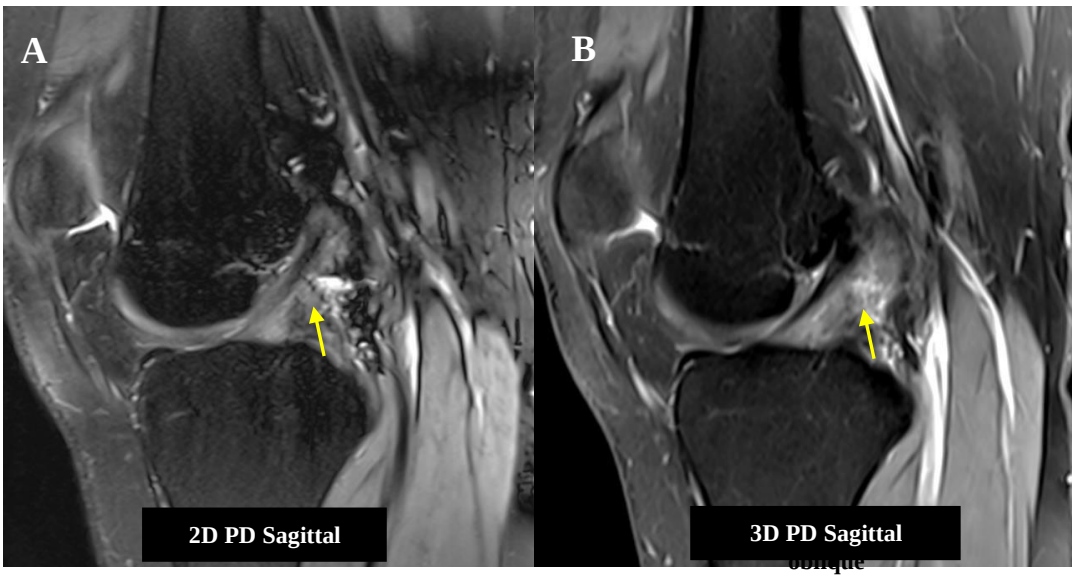

Figure 2: 2D (A) and 3D (B) PD sagittal images with fat suppression of the same patient. 2D PD image (A) revealed blurring of ACL fibres at its distal part, which can be seen intact at the 3D PD sagittal view (B) with adequate improvement in resolution along its entire course compared to the 2D PD image (A). The ACL fibres are sharper in the 3D PD image (score 3) than the 2D PD image (score 1). The injury score was 5 for the 2D image and 4 for the 3D image.

The area under the curve (AUC) was analyzed to evaluate the diagnostic performance of each quantitative measurement for detecting a pathology. Ninety-five percent confidence intervals were considered for all AUC to assess significant changes between the protocols. In addition, to descriptive statistics were employed for direct comparisons.

The sensitivity, specificity, positive predictive value, negative predictive value, and accuracy of both 2D TSE and 3D SPACE sequences in detecting ACL abnormalities were calculated to increase the statistical power of the comparison. All statistical evaluations were performed using the Statistical Package for Social Sciences (SPSS, version 23, Chicago, IBM, IL, USA).

Result

Gender and Age of Subject Distribution

The patients' group consists of 82.9% male and 17.1% female. About 64% of the subjects were male, and 36% were female in the healthy group. The finding reveals no statistically significant association between the participants concerning gender ($\chi 2$= 2.766, p=0.096), as shown in **Table 2.**

Table 2: Descriptive statistics of gender

Gender	Patient numbers (%)	Healthy numbers (%)	$\chi 2$	P-value
Male	29 (82.9 %)	16 (64 %)	2.766	0.096
Female	6 (17.1 %)	9 (36 %)		
Total	35 (100%)	25 (100%)		

The healthy group's age varied from 15 to 55 years old (mean = 36.16, SD = ±10.08). As indicated in **Table 3,** the patient's group ranged from 16 to 55 years old (mean = 33.09 and SD = ± 11.62), without any statistical difference in age between the healthy and the patients (t=1.067, p=0.291).

Table 3: Mean age distribution in healthy and patient groups

Group	Mean ± SD	T-value	P-value
Patient	33.09 ± 11.62	1.067	0.291
Healthy	36.16 ± 10.08		

Image sharpness of the ACL Grading

The result of the inter-observer agreement regarding the image sharpness of the ACL graded between the two observers for each sequence and group is shown in (**Table 4**). Kappa values were interpreted as slight (00.0–0.20), fair (00.21–0.40), moderate (00.41–0.60), substantial (00.61–0.80), or excellent (00.81–1.0). Both observers showed substantial agreement in grading the images sharpness (kappa: 0.688 and 0.651) in the healthy and patient groups, respectively for the 2D images. In addition, both observers showed excellent agreement (kappa: 0.911 and 0.851) in grading the image sharpness of the ACL of the 3D-images in the healthy and patient groups correspondingly.

Table 4: Inter-observer agreement of the ACL margin sharpness between the two observers for both sequences and groups

Sequences	Groups	Kappa	SE
2D	Healthy	0.688	0.129
	Patients	0.651	0.129
3D	Healthy	0.911	0.082
	Patients	0.851	0.101

**SE: standard error*

The ACL sharpness was compared between the 2D and 3D PDW images for each group separately using the U Mann-Whitney test since the variable was of an ordinal type (**Table 5**). **Table 5** shows the mean, standard deviation, and median grade (M) of the ACL sharpness for each sequence and each group. In the healthy group, the median sharpness of the ACL for both the 2D and 3D PDW images was excellent (M=3). In contrast, the ACL sharpness grade in the patients' group between these two sequences was significantly different (p=0.001). The 3D PDW images have an excellent image sharpness of the ACL (M=3) compared to the 2D PDW images (M=2). Comparison between the patient and healthy groups using the U-Mann Whitney test revealed that despite the median of the ACL sharpness grade from the 2D PDW images in the healthy group (M=3) was more than the patient's group (M=2), but it was not significantly different. For the 3D PDW images, the results also showed no significant difference in the ACL sharpness grade between the patient and healthy groups(p=0.438).

Table 5: Comparison of the ACL sharpness grade images between the 2D and 3D sequences image in both groups

Groups	2D-PD TSE Mean ± SD (M)	3D-PD SPACE Mean ± SD (M)	p-value
Healthy	2.52 ± 0.65(3)	2.68 ± 0.48 (3)	0.285
Patients	2.31 ± 0.46 (2)	2.77 ± 0.43 (3)	0.001
P value	0.422	0.438	

ACL Injuries Grading

The types of ACL injuries were evaluated using grades on a scale of 1–5 (Grade 1: normal, Grade2: probably not a tear, Grade 3: indeterminate, Grade 4: partial tear, and Grade 5: complete tear) as show in **Table 6**. Examples of ACL injuries grades shown in **Figure 3, 4 and 5**.

Table 6: Frequency distribution and percentage of healthy and patient's subjects for each types of ACL injury graded by two observers for the 2D PDW and 3D PDW images that acquired using 2D TSE and 3D SPACE sequences

ACL Injury Grades	Observer 1				Observer 2			
	2D TSE		3D SPACE		2D TSE		3D SPACE	
	Healthy	Patients	Healthy	Patients	Healthy	Patients	Healthy	Patients
1	20	-	22	-	23	-	21	-
2	5	-	3	-	2	-	4	-
3	-	-	-	-	-	-	-	-
4	-	18	-	16	-	11	-	12
5	-	17	-	19	-	24	-	23
Total	25	35	25	35	25	35	25	35

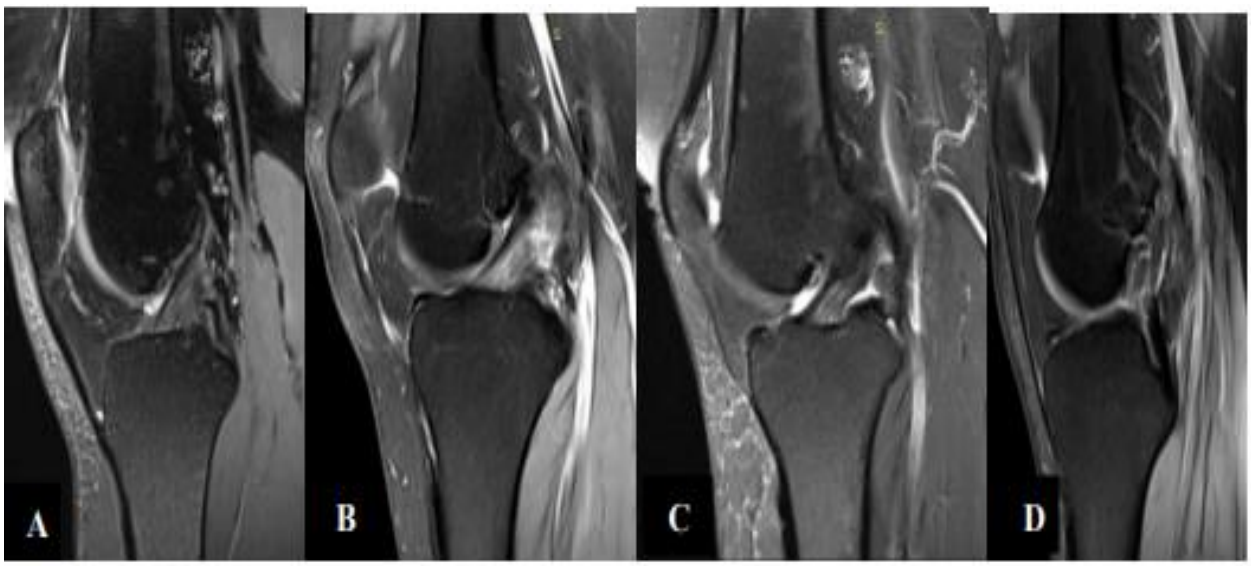

Figure 3: 3D -PD images with fat suppression (FS) of patients with different grades of ACL injury. (A) normal (Grade 1), (B) probably not a tear (Grade 2), (C) partial tear (Grade 4) and (D) complete tear (Grade 5).

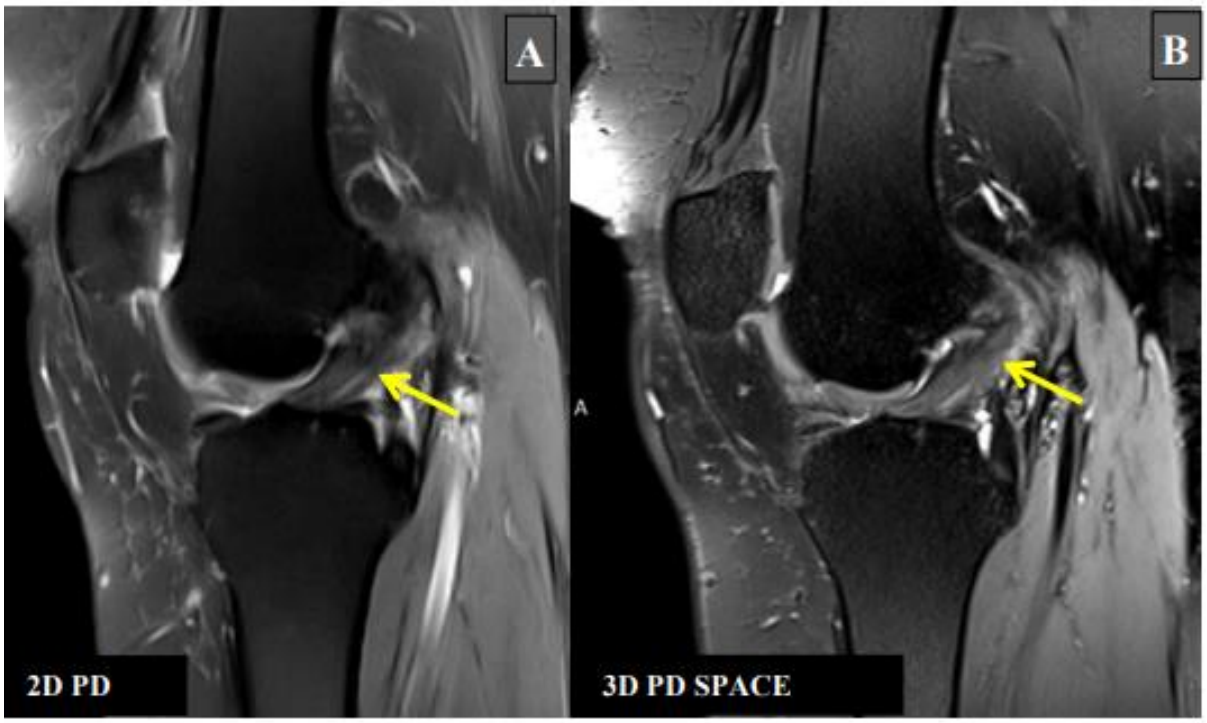

Figure 4: Sagittal images of the knee with fat suppression (FS) of the same patient demonstrate abnormal increases in thickness, intra-substance increased signal intensity of the ACL fibres, and a wavy contour (arrows) denoting a partial tear (score 4) using the 2D TSE (A) and 3D SPACE sequences (B). The 3D PD sagittal view (B) shows a clear improvement in resolution compared to the reference anisotropic low-resolution 2D PD image (A) shown in the left panel.

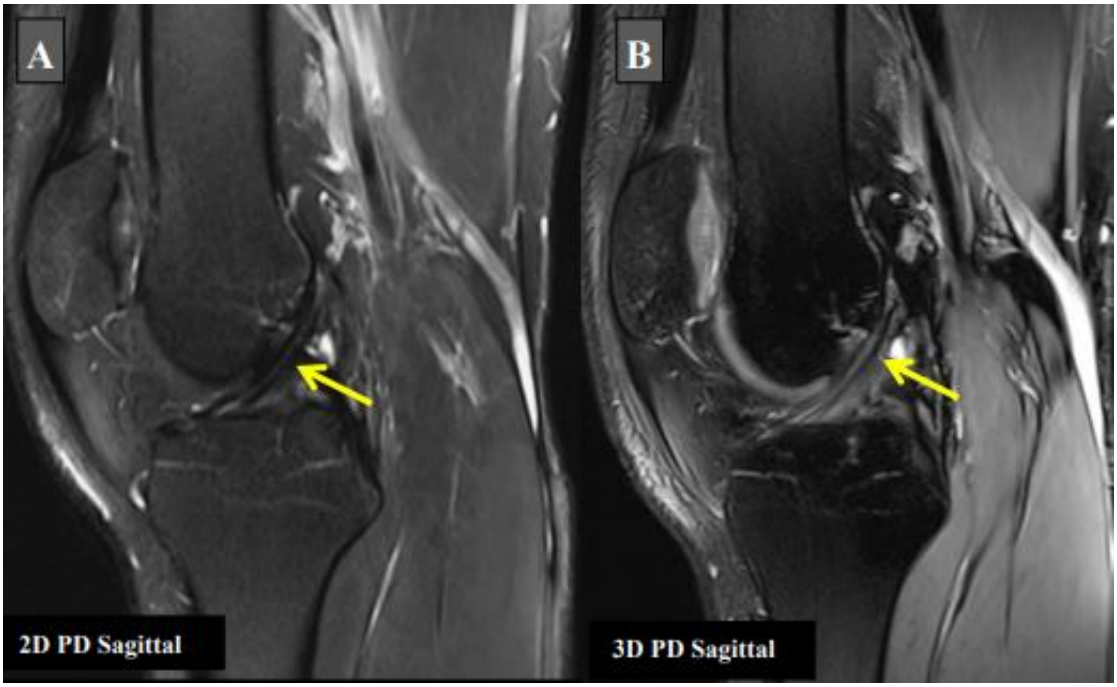

Figure 5*:* Sagittal view of 2D PD image (A) and sagittal oblique view of 3D PD SPACE image (B)MR with fat suppression showing better delineation of the ACL fibres with abnormal high signal intensity inside (arrows), denoting a partial tear (score 4).

Table 7 shows the results from an inter-observer agreement between the two observers for each sequence. For the 2D PD images, both observers showed moderate agreement regarding ACL injuries in both groups with a weighted kappa (k) of 0.516 and 0.557, respectively. For the 3D PDW images, both observers showed excellent agreement in ACL injuries grading in the healthy group with a weighted kappa (k) of 0.834, and moderate agreement in the patient group with a weighted kappa of 0.530.

Table 7: Inter-observer agreement of the ACL injury grading between the two observers for the 2D and 3D PDW images that acquired using the 2D TSE and 3D SPACE sequences.

Sequences	Groups	Kappa	SE
2D-PD	Healthy	0.516	0.229
	Patients	0.557	0.123
3D-PD SPACE	Healthy	0.834	0.160
	Patients	0.530	0.141

Table 8 shows the agreement of the ACL injury grading between the two sequences for each observer. Observer 1 showed substantial and moderate agreement between ACL injuries at 2D PD and 3DPDW image with a weighted kappa (k) of 0.706 and 0.603 in healthy and patient groups respectively. Observer 2 showed substantial agreement between ACL injuries for the 2D and 3D PDW images with a weighted kappa of (k) 0.627 and 0.677 in healthy and patients' groups respectively.

Table 8: Agreement of the ACL injury grading between the 2D and 3D PDW images that acquired using the 2D TSE and 3D SPACE sequences of each observer.

Observers	Groups	Kappa	SE
Observer 1	Healthy	0.706	0.191
	Patients	0.603	0.132
Observer 2	Healthy	0.627	0.235
	Patients	0.677	0.133

Diagnostic Accuracy of the ACL Injuries

Arthroscopy was performed on 35 patients, all of which were confirmed to have an ACL tear,11 of them had a partial tear, and 24 had a complete tear in the ACL. After the procedure, 20 subjects had been operated on, and the remaining 15 patients underwent conservative management. The diagnosis of the ACL injury using MRI with different sequences was compared with the standard gold of arthroscopy for each patient. True negative (TN) indicated the patient with ACL partial tears that detected using MRI and were confirmed in arthroscopy. While false negative (FN) indicated the patient with ACL partial tears that detected using MRI, but the patients were confirmed having ACL complete tear in arthroscopy. True positive (TP) indicated the patient with ACL complete tear that detected using MRI and were confirmed in arthroscopy. While false positive (FP) indicated the patient with ACL complete tear that detected using MRI, but the patients were confirmed having ACL partial tear in arthroscopy. The diagnostic accuracy was compared between MRI techniques (2D TSE and 3D SAPCE sequences) and arthroscopy as shown in (**Table 9 and Table 10**).

Table 9: Comparison in diagnostic accuracy of ACL injuries between MRI technique (2D TSE) and arthroscopy. The numbers correspond to the number of patients with ACL partial and complete tear.

MRI (2D TSE)	Arthroscopy		Total
	Partial tear (Negative)	Complete tear (Positive)	
Partial tear (Negative)	8 (TN)	3 (FN)	11
Complete tear (Positive)	3 (FP)	21 (TP)	24
Total	11	24	35

Table 10: Comparison in diagnostic accuracy of ACL injuries between MRI technique (3D SPACE) and arthroscopy. The numbers correspond to the number of patients with ACL partial and complete tear.

MRI (3D SPACE)	Arthroscopy		Total
	Partial tear (Negative)	Complete tear (Positive)	
Partial tear (Negative)	10 (TN)	2 (FN)	12
Complete tear (Positive)	1 (FP)	22 (TP)	23
Total	11	24	35

ROC analysis was applied to assess the diagnostic accuracy of both MRI techniques, 2D TSE and 3D SPACE for ACL injuries detection. The ROC curve is a common method to assess accuracy, and it was used to determine the diagnostic accuracy between a partial and complete ACL tear in the patients group.

Results of the ROC analysis (**Table 11**) of the ACL injuries using the 2D TSE and 3D SPACE showed higher AUC for the 3D-PD SPACE (AUC=0.973 with p-value <0.001) compared to the 2D sequence (AUC=0.927 with p-value <0.001), causing a statistical significance.

Table 11: The ROC analysis for the ACL injuries using the 2D TSE and 3D SPACE.

Sequences	Area	SE a	P-Value b	Asymptotic 95% Confidence Interval	
				Lower Bound	Upper Bound
2D-PD TSE	0.927	0.032	<0.001	0.864	0.990
3D-PD SPACE	0.973	0.020	<0.001	0.933	1.000

a. Under the nonparametric assumption

b. Null hypothesis: true area = 0.5

The AUC for the ACL injuries presented in **Figure 6** indicates that the injury score for both the 2D-PD and 3D-PD SPACE is away from the reference line, meaning a good accuracy for discriminating ACL injuries.

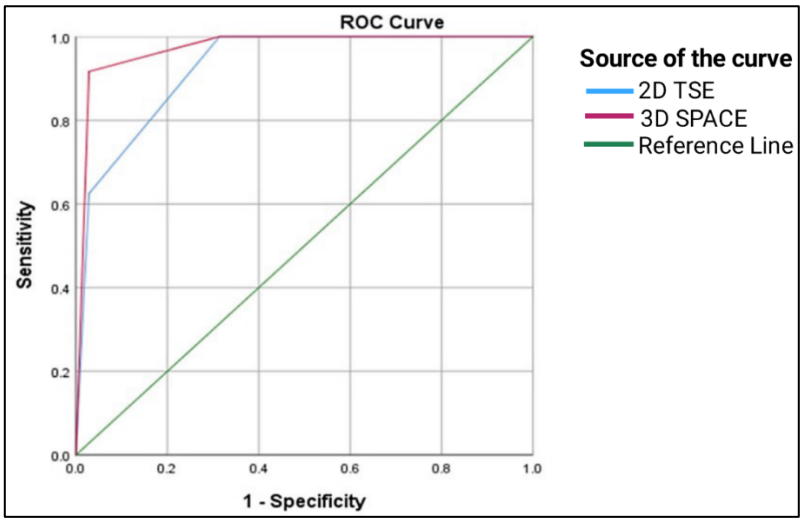

Figure 6: ROC curve of the partial and complete tears of ACL using the 2D-PD and 3D-PD SPACE

The radiological diagnosis of the ACL injury using both the 2D TSE and 3D SPACE sequences were correlated with arthroscopy. The sensitivity and specificity of the 3D SPACE sequence to diagnose anterior cruciate ligament were 91.7% and 90.9% respectively. The positive predictive value of 2D-PD TSE and 3D-PD SPACE sequences, in diagnosis of ACL injuries were 87.5% and 95.7% respectively. The negative predictive value of 2D-PD TSE and 3D-PD SPACE sequence in diagnosis of ACL injuries were 72.7% and 83.3% respectively. **Table 12** shows the statistical correlation of both the MRI techniques and arthroscopy for the ACL tears.

The diagnostic accuracy of ACL injuries using the 3D SPACE sequence was higher than that of the 2D TSE sequence (91.4% versus 82.9%). There was moderate and substantial agreement between the ACL injuries using both MRI sequences and arthroscopy with a weighted kappa (k) of 0.536 and 0.682 respectively (**Table 12**).

Table 12: Statistical correlation between the 2D TSE and 3D SPACE with arthroscopy for ACL partial and complete tears.

Test	2D TSE	3D SPACE
Sensitivity	87.5%	91.7%
Specificity	72.7%	90.9%
Positive predictive value (PPV)	87.5%	95.7%
Negative predictive value (NPV)	72.7%	83.3%
Accuracy	82.9%	91.4%
Kappa (k)	0.536	0.682

Discussion

The anterior cruciate ligament (ACL) is a vital intra-articular stabilizing component of the knee that resists anterior tibial translational and rotational loads. It is a crucial structure in the knee joint and one of the most frequently injured. Magnetic resonance imaging (MRI) has been shown to be a highly accurate, non-invasive tool for assessing ACL injuries (Chen et al., 2013). Ongoing advancements in MRI have led to the introduction of various 3D pulse sequences aimed at enhancing image quality, diagnostic effectiveness, and

simplifying sequence planning. However, the commonly used 2D technique requires precise preparation of imaging planes in different orientations (Van Dyck et al., 2012b). The scanning time for 3D MRI was longer than for 2D methods; however, this may be offset by the ability to perform reformatting in multiple planes, eliminating the need for multiple 2D image acquisitions. Therefore, the total acquisition time for 3D sequences is less than that for 2D sequences. In this study, the 3D-PD-SPACE sequence was utilized as an alternative to the routine 2D-PD TSE protocol, which has the potential to reduce examination time by excluding the T1-weighted sequence (Van Dyck et al., 2012b). To shorten the scan time, the 3D-PD SPACE sequence utilizes variable flip angles modulation by refocusing radiofrequency angle technique, parallel imaging in both the slice-encoding direction and plane, and partial-Fourier acquisition (Busse et al., 2006). A transmit-receive (T/R)-knee coil with increased signal-to-noise ratio (SNR) and multiple elements was utilized at a field strength of 3T to enable the implementation of these techniques. The outcome is a higher SNR, sharper pulse profiles, and shorter pulse durations (Bachschmidt et al., 2015). The latter two points are particularly crucial for turbo spin echo sequences with long echo trains, where limiting the total echo train length is essential to prevent blurring, signal loss, and contrast loss.

Early 3D techniques used gradient echo (GE) sequences, which not only suffered from long scan times but also proved inadequate for accurately assessing ligaments, menisci, and bone marrow changes. These shortcomings were later addressed and rectified by the introduction of 3D-TSE techniques (Crema et al., 2011; Van Dyck et al., 2012b). However, 3D acquisition with the TSE technique is designed for diagnostic purposes. 3D TSE acquisitions can achieve isotropic voxel dimensions and imaging times like those of 3D GE acquisitions (Altahawi et al., 2017). 3D TSE imaging of the knee, with multiplanar reformations and isotropic voxel dimensions, has the potential to replace the multiple conventional 2D protocols currently used for assessing cartilage, menisci, ligaments, and bone marrow edema (Crema et al., 2011; Van Dyck et al., 2012b).

The 3D MRI produces high-quality volumetric images. These images can be reformatted to any orientation without any additional acquisitions to obtain specific angulations that are essential for visualizing small knee structures (Henninger et al., 2018a; Subhas et al., 2011a). By acquiring only a set of images, it allows for the assessment of the knee in all three anatomical orientations and the evaluation of oblique structures (such as the anterior cruciate ligament) by reconstruction along the areas of interest (Henninger et al., 2018b). However, it is still unclear whether only one 3D TSE acquisition can replace multiple conventional 2D acquisitions commonly used in clinics (Rajeswaran et al., 2007). Other significant advancements have been made at higher field strengths, such as the 3T scanner using parallel imaging, non–frequency-selective refocusing pulses, and multi-channel surface coils, which have also improved image quality and reduced scan times while maintaining good signal-to-noise ratios [15].

In this study, the diagnostic performance of the ACL was evaluated based on the ACL visualization of anatomical details and injuries on the Proton Density Weighted (PDW) images acquired using 2D TSE and 3D. We found 3D SPACE offers high-quality of PDW images of the ACL with nearly comparable and in contrast to 2D TSE. Notohamiprodjo et al. (2012) reported that enhanced 3D SPACE sequence gives higher signal and contrast as when compared to conventional 2D sequences, refining diagnostic confidence. They also reported that the detection and visualization of knee pathologies by 3D PDSPACE are comparable to standard 2D TSE sequences [16]. [17] found that both conventional 2D TSE and isotropic 3D SPACE protocols were similar in the assessment of the knee ligaments, which was in line with our results.

There was substantial agreement in grading ACL sharpness for the healthy and patient' groups between two observers for 2D TSE sequences in this study. However, the 3D SPACE sequence showed excellent agreement between both observers in grading ACL sharpness for healthy and patient' groups. Park et al. (2016) reveal that the ACL image sharpness with the 2D FSE and 3D sequence techniques evaluated by the two radiologists revealed excellent reproducibility, comparable to our results. They found that interobserver agreement for the 3D sequence was equal to that of 2D FSE (Homsi et al., 2016). Park et al. (2016) testified that, though the image quality of the 3D sequence was lesser than that of 2D FSE, the diagnostic value of

the oblique sagittal and oblique coronal 3D images was like that of 2D images (Homsi et al., 2016). We found that the mean sharpness of the margin of the ACL was excellent in the 3D PDW images compared to 2D PDW images in patients with ACL injury, and the difference was statistically significant. The improved sharpness of ACL edge by 3D SPAC in this study may be attributed to a small slice thickness (0.45 mm). Though the capacity to visualize the whole length of the ACL was comparable between the two techniques, Park et al. (2016) found that the 3D images had less image sharpness compared with 2D FSE images. Ristow et al. (2009) reported less sharpness with the 3D FSE result than with the 2D FSE images. The inferior sharpness in 3D images may be related to reconstruction with a larger slice thickness. Homsi et al. (2016) reported higher sharpness in 2D-PD than 3D-PD in corresponding planes, which was different from our results. This might be ascribed to the lower in-plane resolution of the 3D-PD as compared to the 2D-PD images in their study (Henninger et al., 2018).

There was moderate agreement in grading ACL injuries for patients with ACL injury between two observers for both sequences. However, there was substantial agreement in grading ACL injuries for healthy and patient groups between 2D and 3D sequences for each observer. Jung et al. (2013) equated a 3D isotropic TSE acquisition with 2D TSE MRI for the performance in the diagnosis of internal instabilities of the knee. They also observed no significant changes in sensitivity, specificity, nor accuracy between the two protocols with exceptional interobserver agreement for the assessment of all alterations (Jung et al., 2013). Furthermore, their study excluded the assessment of cartilage altogether, as in this study.

In this study, 2D TSE and 3D SPACE revealed almost similar sensitivity, specificity, and diagnostic accuracy in the evaluation of ACL partial and complete tears; 3D SPACE had slightly higher sensitivity and specificity than 2D TSE. Therefore, we concluded that 3D SPACE is effective in assessing ACL injuries compared to the 2D TSE sequence. This result differed from the findings reported by Homsi et al. (2016), who noted no differences between the two sequences in lesion detection. Homsi et al. (2016) found no significant difference between both protocols, possibly due to limitations in their study, such as a small sample size and a limited number of patients referred for arthroscopy. Ristow et al. (2009) also noted that the diagnostic performance of the 3D FSE sequence was lower than that of the standard 2D FSE sequence, primarily due to the low image quality of the reconstructions, which greatly hindered the visualization of anatomical structures despite selecting a 2-mm slice thickness for image reformatting. Van Dyck et al. (2012) similarly reported that the diagnostic performance of the 3D sequence was inferior to the 2D sequence in evaluating the patellofemoral compartment. The 3D SPACE sequence offers advantages over 2D sequences for assessing knee ligaments. The thin sections of 3D SPACE reduce partial-volume averaging, a potential cause of diagnostic errors in assessing the ACL of the knee. Although in this study, 3D SPACE demonstrated comparable sensitivity, specificity, and accuracy to the routine 2D TSE sequence in detecting ACL tears, consistent with the results of Van Dyck et al. (2012), Cao et al. (2015), and Rajeswaran et al. (2007). However, initial observations on the diagnostic performance of 3D isotropic resolution were promising, but recent studies have highlighted the limitations of these sequences due to small sample sizes and a limited number of patients for assessing the knee joint [15].

Van Dyck et al. (2012b) assessed the diagnostic performance of a 3D SPACE TSE sequence and compared it to a 2D TSE on a knee joint using 3T. In their study, arthroscopy served as the reference standard, revealing improved findings with the 2D technique for the medial meniscus; however, both techniques demonstrated similar performance for the rest. In contrast to our results, they concluded that the traditional 2D protocol is more reliable than the 3D SPACE. It is noteworthy that Van Dyck et al. (2012b) utilized an 8-channel knee coil and a non-optimized SPACE sequence. Another advantage of 3D SPACE is the potential reduction in preparation time for the MR radiologist, as precise angulations along small anatomic structures are unnecessary when acquiring extensive 3D data sets (Mallio et al., 2023). The relatively lengthy acquisition time of the 3D SPACE sequence could result in motion artifacts.

In the 3D-PD image acquisition, brief patient movements may disturb the entire 3D data set. In this situation, repeating the 3D-PD sequence is more

time-consuming than repeating a single 2D-PD plane that was acquired during the short movement phase. In these specific scanning, prolongation of total scan time is viewed as a likely weakness of the 3D technique [19].

There were limitations encountered in this study. Firstly, there were insufficient participants enrolled in the study. The study was very important clinical research, although it involved a small number of samples in both the normal and injured patients, which is below the minimum sample size to have an effect size variation between the sequences. However, casual fluctuations could cause changes in MR accuracy, which can occur even with a large population enrolled in the study. It was obvious that without reaching any statistically significant differences, our present work reveals clinically significant findings indicating that 3D SPACE is an excellent tool, although without a superior sequence as compared to recently employed 2D sequences for diagnosing ACL lesions. Second, in this study, sequences were compared with diverse slice thicknesses and spatial resolutions. Although reconstructing 3D SPACE images was not of major interest with a larger slice thickness since we needed to evaluate the great potential of the small slice thickness. However, according to the works of Notohamiprodjo et al. (2012b), it was reported that 3D SPACE with 1-mm MPRs was superior to 3D SPACE with 2-mm MPRs for visualization of anatomic structures.

Furthermore, the non-randomized sequence order was considered a limitation in this study. In unstable patients unable to tolerate long acquisition trials, motion artifacts are more likely to be present. However, the final image quality was rated higher in the 3D SPACE sequence acquired second, supporting the non-inferiority findings of 3D-PD. Nonetheless, we did not observe any instances of decreased diagnostic image quality.

Based on our findings, we believe that this work adds to the growing pool of data signifying that 3D PD SPACE might be a valuable and reliable constituent of a knee MR protocol at 3T. The 3D PD SPACE was shown to provide sufficient image quality comparable to that of a conventional 2D PD TSE sequence in a realistic scan time. Isotropic data from the 3D PD SPACE sequence allows for multiplanar reformatting in arbitrary planes, causing multiple 2D acquisitions unnecessary.

The primary finding in this study is that the 3D PD SPACE sequence produced excellent sharpness of the ACL in 3D PDW images, compared to the 2D PDW images (M=2) used for evaluating ACL injuries in patients, while also demonstrating higher reliability. Moreover, this sequence exhibits excellent diagnostic accuracy for ACL injuries but with moderate reliability. Therefore, the 3D PD SPACE sequence may offer advantages over the 2D TSE sequence for assessing anterior cruciate ligament injuries. The thin, continuous slices of the 3D PD SPACE sequence minimize the impact of partial-volume averaging, which could lead to diagnostic errors when examining the ACL of the knee. We suggest using this sequence as a complement to the standard 2D sequences, as it proves valuable in assessing high-contrast structures. However, further studies are necessary to evaluate the image quality and diagnostic performance of the 3D PD SPACE sequence in knee MR protocols at 3 T. With additional optimization, the 3D PD SPACE sequence reformatted into multiple planes could potentially serve as a substitute for separately acquired 2D TSE sequences, significantly reducing the overall examination time.

Conclusion

In conclusion, this finding augments the growing evidence indicating that the 3D PD SPACE sequence may be a dependable constituent of knee MR techniques at 3T. The 3D-PD SPACE sequence offers satisfactory image quality comparable to that of the 2D-PD sequence at a reasonable scan time. We recommend using this sequence as a supplementary sequence since it is found to be valuable in evaluating high-contrast structures. The quality of images and diagnostic performance of the 3D PD SPACE sequence in 3T knee MR operations will require more investigation.

Abbreviations

3D	Three-dimensional
2D	Two-dimensional
3D SPACE	Three-dimensional Sampling Perfection with application – optimized contrasts using variable flip angle evolution

2D TSE	Two-dimensional Turbo Spin Echo
ACL	Anterior Cruciate Ligament
3T MRI	3.0 Tesla Magnet Scanner Magnetic Resonance Imaging
2D PD	Two-dimensional Proton density
3D PD	Three-dimensional Proton density
MRI	Magnetic Resonance Imaging
ROI	Region of interest
ACL	Anterior cruciate ligaments
3D isotropic FSE	Three-dimensional Isotropic Fast Spin Echo
FS	Fat-Suppressed
PD	Proton Density
PDW	Proton Density Weighted
AUC	Area Under the Curve
SD	Standard Deviation
PPV	Positive Predictive Value
NPV	Negative Predictive Value
FSE	Fast Spin Echo
T1W	T1-weighted
T2W	T2-weighted
P value	Probability value

Acknowledgment

The authors are thankful to the King Fahd Hospital and University Putra Malaysia (UPM), for this research study's continuous support.

Author contributions

All authors read and approved the final manuscript.

Funding

The study has no funding from any resources.

Availability of data and materials

The datasets used and/or analyzed during the current study are available from the corresponding author upon reasonable request.

Ethical Consideration

Ethical approval was obtained from King Fahd Hospital and the University Putra Malaysia (UPM) ethical review committees. The data was only used in this study after acquiring informed written consent from the participants to be examined by MRI. According to the Saudi Ministry of Health for Scientific Research regulations, all participants' data were verified. The approval of the competent committee for clinical trials was obtained according to the following ethical approvals: IRB340 and JKEUPM-2019-451, respectively. The names or information indicating the participants were not published, and the information was kept strictly confidential inside the facility.

Conflict of interest

The authors declare that there is no conflict of interest**.**

Authors contribution

AAD, NFO & MS Conceptualized the study, developed the research methodology, and supervised the overall project. Contributed to data interpretation and manuscript writing. AAD Conducted data collection, performed the experiments and analyzed the results. Prepared the initial draft of the manuscript. ACA: Assisted with data curation, contributed to statistical analyses, and participated in revising the manuscript for critical intellectual content. AAD, NFO , DA, & MS reviewed and approved the study design, and critically reviewed the manuscript. AI, HAA, THA: Assisted with project administration, provided technical expertise, and participated in the final review and approval of the manuscript. All authors read and approved the final manuscript.

References

[1] A. J. Wiggins, R. K. Grandhi, D. K. Schneider, D. Stanfield, K. E. Webster, and G. D. Myer, “Risk of Secondary Injury in Younger Athletes after Anterior Cruciate Ligament Reconstruction,” 2016. doi: 10.1177/0363546515621554.

[2] N. C. Nacey, M. G. Geeslin, G. W. Miller, and J. L. Pierce, “Magnetic resonance imaging of the knee: An overview and update of conventional and state of the art imaging,” *Journal of Magnetic Resonance Imaging*, vol. 45, no. 5, 2017, doi: 10.1002/jmri.25620.

[3] C. G. Fazio, P. Muir, S. L. Schaefer, and K. R. Waller, "Accuracy of 3 Tesla magnetic resonance imaging using detection of fiber loss and a visual analog scale for diagnosing partial and complete cranial cruciate ligament ruptures in dogs," *Veterinary Radiology and Ultrasound*, vol. 59, no. 1, 2018, doi: 10.1111/vru.12567.

[4] J. Hossein, F. Fariborz, R. Mehrnaz, and R. Babak, "Evaluation of diagnostic value and T2-weighted three-dimensional isotropic turbo spin-echo (3D-SPACE) image quality in comparison with T2-weighted two-dimensional turbo spin-echo (2D-TSE) sequences in lumbar spine MR imaging," *Eur J Radiol Open*, vol. 6, 2019, doi: 10.1016/j.ejro.2018.12.003.

[5] C. Tippareddy, W. Zhao, J. L. Sunshine, M. Griswold, D. Ma, and C. Badve, "Magnetic resonance fingerprinting: an overview," 2021. doi: 10.1007/s00259-021-05384-2.

[6] S. Mastrogiacomo, W. Dou, J. A. Jansen, and X. F. Walboomers, "Magnetic Resonance Imaging of Hard Tissues and Hard Tissue Engineered Bio-substitutes," 2019. doi: 10.1007/s11307-019-01345-2.

[7] B. Pass, P. Robinson, R. Hodgson, and A. J. Grainger, "Can a single isotropic 3D fast spin echo sequence replace three-plane standard proton density fat-saturated knee MRI at 1.5T?," *British Journal of Radiology*, vol. 88, no. 1052, 2015, doi: 10.1259/bjr.20150189.

[8] P. Van Dyck *et al.*, "Diagnostic performance of 3D SPACE for comprehensive knee joint assessment at 3 T," *Insights Imaging*, vol. 3, no. 6, 2012, doi: 10.1007/s13244-012-0197-5.

[9] K. Amano, Q. Li, and C. B. Ma, "Functional knee assessment with advanced imaging," 2016. doi: 10.1007/s12178-016-9340-0.

[10] K. L. Fleming, T. W. Maddox, and C. M. R. Warren-Smith, "Three-dimensional T1-weighted gradient echo is a suitable alternative to two-dimensional T1-weighted spin echo for imaging the canine brain," *Veterinary Radiology and Ultrasound*, vol. 60, no. 5, 2019, doi: 10.1111/vru.12774.

[11] H. J. Park *et al.*, "Three-dimensional isotropic T2-weighted fast spin-echo (VISTA) knee MRI at 3.0 T in the evaluation of the anterior cruciate ligament injury with additional views: Comparison with two-dimensional fast spin-echo T2-weighted sequences," *Acta radiol*, vol. 57, no. 11, 2016, doi: 10.1177/0284185114568048.

[12] J. Fritz, E. Raithel, G. K. Thawait, W. Gilson, and D. F. Papp, "Six-fold acceleration of high-spatial resolution 3D SPACE MRI of the knee through incoherent k-space undersampling and iterative reconstruction - First experience," *Invest Radiol*, vol. 51, no. 6, 2016, doi: 10.1097/RLI.0000000000000240.

[13] D. Shakoor *et al.*, "Diagnostic performance of three-dimensional MRI for depicting cartilage defects in the knee: A meta-analysis," *Radiology*, vol. 289, no. 1, 2018, doi: 10.1148/radiol.2018180426.

[14] M. B. Appayya, E. W. Johnston, and S. Punwani, "The role of multi-parametric MRI in loco-regional staging of men diagnosed with early prostate cancer," 2015. doi: 10.1097/MOU.0000000000000215.

[15] R. Homsi *et al.*, "Three-Dimensional Isotropic Fat-Suppressed Proton Density-Weighted MRI at 3 Tesla Using a T/R-Coil Can Replace Multiple Plane Two-Dimensional Sequences in Knee Imaging," *RoFo Fortschritte auf dem Gebiet der Rontgenstrahlen und der Bildgebenden Verfahren*, vol. 188, no. 10, 2016, doi: 10.1055/s-0042-111826.

[16] M. Notohamiprodjo *et al.*, "3D-MRI of the ankle with optimized 3d-space," *Invest Radiol*, 2012, doi: 10.1097/RLI.0b013e31823d7946.

[17] N. Subhas, A. Kao, M. Freire, J. M. Polster, N. A. Obuchowski, and C. S. Winalski, "MRI of the knee ligaments and menisci: Comparison of isotropic-resolution 3D and conventional 2D fast spin-echo sequences at 3 T," *American Journal of Roentgenology*, 2011, doi: 10.2214/AJR.10.5709.

[18] P. Van Dyck *et al.*, "Diagnostic performance of 3D SPACE for comprehensive knee joint assessment at 3 T," *Insights Imaging*, 2012, doi: 10.1007/s13244-012-0197-5.

[19] C. A. Mallio *et al.*, "Advanced MR Imaging for Knee Osteoarthritis: A Review on Local and Brain Effects," 2023. doi: 10.3390/diagnostics13010054.